The Astronomical Journal, 125:984–993, 2003 February

THE USNO-B CATALOG

David G. Monet, Stephen E. Levine, Blaise Canzian, Harold D. Ables,[1] Alan R. Bird,[1] Conard C. Dahn, Harry H. Guetter,[1] Hugh C. Harris, Arne A. Henden,[2] Sandy K. Leggett,[3] Harold F. Levison,[4] Christian B. Luginbuhl, Joan Martini, Alice K. B. Monet, Jeffrey A. Munn, Jeffrey R. Pier, Albert R. Rhodes, Betty Riepe, Stephen Sell, Ronald C. Stone, Frederick J. Vrba, Richard L. Walker,[1] and Gart Westerhout[1]
US Naval Observatory, Flagstaff Station, P.O. Box 1149, Flagstaff, AZ 86002

Robert J. Brucato and I. Neill Reid[5]
Palomar Observatory, 105-24, California Institute of Technology, 1201 East California Boulevard, Pasadena, CA 91125

William Schoening[1]
National Optical Astronomy Observatory, 950 North Cherry Avenue, Tucson, AZ 85719

M. Hartley
UK Schmidt Telescope, Anglo-Australian Observatory, Coonabarabran, NSW 2357, Australia

and

M. A. Read and S. B. Tritton
Royal Observatory Edinburgh, Blackford Hill, Edinburgh EH9 3HJ, Scotland, UK
Received 2002 October 11; accepted 2002 October 31

ABSTRACT

USNO-B is an all-sky catalog that presents positions, proper motions, magnitudes in various optical passbands, and star/galaxy estimators for 1,042,618,261 objects derived from 3,643,201,733 separate observations. The data were obtained from scans of 7435 Schmidt plates taken for the various sky surveys during the last 50 years. USNO-B1.0 is believed to provide all-sky coverage, completeness down to $V = 21$, $0\farcs2$ astrometric accuracy at J2000, 0.3 mag photometric accuracy in up to five colors, and 85% accuracy for distinguishing stars from nonstellar objects. A brief discussion of various issues is given here, but the actual data are available from the US Naval Observatory Web site and others.

Key words: astrometry — catalogs

1. INTRODUCTION

The USNO-B catalog, currently released in version 1.0, is compiled from the digitization of various photographic sky survey plates by the Precision Measuring Machine (PMM), located at the US Naval Observatory Flagstaff Station (NOFS). The PMM produces both a pixel archive and a list of detections for each plate in real time. The plate material includes five complete coverages of the northern sky and four of the southern sky and contains a mixture of colors and epochs. The catalog was compiled from the merged lists of detections and presents position, proper motion, magnitudes in various colors, star/galaxy classification, and various uncertainty estimators for 1,042,618,261 distinct objects. A discussion of the technical details is presented in the documentation associated with the catalog and, like the catalog, is not being submitted for publication in the literature.[6]

USNO-B is the next step in the sequence of catalogs that started with UJ1.0 (Monet et al. 1994), USNO-A1.0 (Monet et al. 1996), and USNO-A2.0 (Monet et al. 1998). In simple terms, USNO-A was a two-color, one-epoch catalog, while USNO-B is a three-color, two-epoch catalog. However, this simplification is not entirely correct. The southern surveys that were part of USNO-A were taken at two epochs, and there is no first-epoch blue survey south of $\delta = -33^\circ$ to include in USNO-B. For both catalogs, an object must be detected on two different surveys to be included, since isolated, single-survey detections are unreliable. For USNO-A, this meant that the object must have had detectable red and blue fluxes, and this led to the exclusion of many faint objects with nonneutral colors. Also, the epoch difference in the southern surveys meant that objects with larger proper motions tended to be excluded. USNO-B attempts to fix both of these problems. An object detected on the same color survey at two epochs will be included in USNO-B, as will objects that have significant proper motions, although it is still the case that objects with large motions and extreme colors may be omitted. The selection algorithm requires that spatially coincident detections must be made on any two of the surveys for an object to be classified as real and be included in the catalog.

2. PLATE MATERIAL

Even in these modern times, one cannot help but be impressed by the effort and dedication put into the photographic sky surveys. A useful overview was presented by Morgan et al. (1992), and Table 1 presents the general properties of the surveys incorporated into USNO-B. The following details are of general interest, but the rest are

[1] Retired.
[2] Universities Space Research Association.
[3] Joint Astronomy Centre, 660 North A'ohoku Place, Hilo, HI 96720.
[4] Department of Space Studies, Southwest Research Institute, Suite 400, 1050 Walnut Street, Boulder, CO 80302.
[5] Space Telescope Science Institute, 3700 San Martin Drive, Baltimore, MD 21218.
[6] The digital distribution can be found at http://www.nofs.navy.mil and other sites.

TABLE 1
PHOTOGRAPHIC DATA

Survey	Emulsion	Wavelength (nm)	Declination[a]	Fields	Epoch[b]	Archive[c]
POSS-I	103a-O	350–500	−30 to +90	936	1949–1965 (first)	O
	103a-E	620–670	−30 to +90	936	1949–1965 (first)	O
POSS-II	IIIa-J	385–540	0 to +87.5	897	1985–2000 (second)	O
	IIIa-F	610–690	0 to +87.5	897	1985–1999 (second)	O
	IV-N	730–900	+5 to +87.5	800	1989–2000	O
SERC-J	IIIa-J	395–540	−90 to −20	606	1978–1990 (second)	G
SERC-EJ	IIIa-J	395–540	−15 to −5	216	1984–1998 (second)	G
ESO-R	IIIa-F	630–690	−90 to −35	408	1974–1987 (first)	G
AAO-R	IIIa-F	590–690	−90 to −20	606	1985–1998 (second)	O
SERC-ER	IIIa-F	590–690	−15 to −5	216	1979–1994 (second)	G
SERC-I	IV-N	715–900	−90 to 0	892	1978–2002	O
SERC-I[d]	IV-N	715–900	+5 to +20	25	1981–2002	O

NOTE.—References for the individual surveys can be found in Morgan et al. 1992, and the wavelength data presented above were copied from this source.

[a] Range of field centers in nominal B1950 used in the compilation of USNO-B. In many cases, the survey covers a larger area.

[b] The assignment of first or second epoch is used in the compilation of the catalog. In this notation, there is no first-epoch blue survey south of $\delta = -33^\circ$.

[c] "O" is the original plate, "G" is the glass copy. In isolated cases, a glass copy was scanned when the original plate was found to be broken, missing, or otherwise unacceptable. For surveys marked with G, the glass copies were borrowed from the National Optical Astronomy Observatory.

[d] Extension of SERC-I survey to fill holes in POSS-II IV-N survey.

relegated to the documentation associated with the digital version of the catalog:

In perhaps 20 cases, the original plate (mostly in POSS-I) has disappeared and cannot be found. In these cases, the glass copy was scanned.

It appears to take about 15 years to complete a photographic survey. The epoch for a particular field can be quite different from the mean epoch, and this difference can be quite important in the measurement of stellar proper motions.

The total number of plates included in USNO-B1.0 is 7435. The missing fields are numbers 1 and 646 in the SERC-I survey. These were not available in time for this release but will be included in later releases.

In our notation, there are 937 POSS-I fields. The centers for fields 1 and 2 and for fields 723 and 724 are the same. Both fields 1 and 2 are included, since they were taken at very different hour angles (they are at the north celestial pole), but field 723 was omitted because 724 was published in the atlas. As a result of these degeneracies, different numbering schemes have been used over the years, and some confusion persists.

The plates involved in USNO-B are about 60% of the Schmidt plates scanned by the PMM. Data from the other plates (rejected, Luyten's, etc.) will be included in future USNO catalogs.

3. SCANNING PROCEDURE

The PMM differs from most other astronomical plate scanners because it uses a two-dimensional charge-coupled device (CCD) camera as its sensor. A Schmidt plate is digitized in 588 separate exposures, and each produces a 1312×1032 image digitized with 8 bit resolution. The CCDs have 6.8 μm $\times$ 6.8 μm pixels and a 100% fill factor, and they are read at 10 million pixels per second. A complete exposure cycle takes about 0.5 s, including the shutter operation and integration times. A lens provides 2 : 1 imaging of the CCD on the focal plane. Using a nominal plate scale of $67'' \text{ mm}^{-1}$, the pixels are about $0''.9$ in size, the field of view is about $20' \times 15'$, and the spacing between exposures is about $18' \times 13'$. The PMM has two CCD camera systems, but mechanical limitations restrict parallel operations to about 60% of each plate.

The PMM is also different from other scanners because all image processing is done in real time. Each CCD is connected to a computer by an optical fiber and a DMA (direct memory access) interface, and each frame is fully archived and processed before the next is taken. The processing is quite complicated; a detailed description (including source code) is included in the USNO-B documentation, but the following gives the major steps. After the data arrive in physical memory, the process forks and one path writes the raw data to magnetic tape and then exits. The processing path starts with bias removal, flat-field correction, and an object finder. Each object is processed in steps of increasing precision, but the processing of each object is independent of all others. This independence enables the usage of parallel processing by the four CPUs in each computer and was a necessary simplification given the computers available in the early 1990s. Table 2 lists all of the parameters computed for each object in every frame. This rich parameter set obviates the need to make a "star" or "galaxy" decision in real time. Once the entire plate has been scanned, the list of object parameters is flushed first to disk, and then (off-line) to CD-ROM. All data in USNO-B come from these files, and the look-back index given for each detection in the catalog allows all quantities to be recovered from the database.

Perhaps the only portion of the algorithm worthy of comment here is the one used to compute the image position. The image data are 8 bits in transmission, and by measuring photographic negatives, the sky is bright and the images are faint. Since most of the survey plates are lacking density calibration spots or wedges, and because the scattered light

TABLE 2
PMM Image Parameters

Name	Description	Range of Values
NFit.....	Total number of pixels in fit	0–9999
NSat	Number of saturated pixels in fit	0–9999
CCDX	Integer X (column) pixel	0–9999
CCDY	Integer Y (row) pixel	0–9999
Frame	Frame count into scan	0–999
A.....	Amplitude of fit	−99.9 to 899.9
B.....	Background of fit	−99.9 to 899.9
x_0	X position on plate from fit	0.00–999,999.99
y_0	Y position on plate from fit	0.00–999,999.99
r_0^2.....	Saturation radius from fit	0.0–999.9
α	Wing scale length from fit	0.0–999.9
σ	Standard deviation of fit	0.0–999.9
Mag	log (sum of flux in pixels in fit)	0.00–99.99
M9	log (sum of flux in central 3 × 3 pixels)	0.00–99.99
M00	Image moment log ($\sum wx^0y^0$)	0.00–9.99
M10	Image moment log ($\sum wx^1y^0$)	0.00–9.99
M01	Image moment log ($\sum wx^0y^1$)	0.00–9.99
M20	Image moment log ($\sum wx^2y^0$)	0.00–9.99
M11	Image moment log ($\sum wx^1y^1$)	0.00–9.99
M02	Image moment log ($\sum wx^0y^2$)	0.00–9.99
MR+1	Image moment log ($\sum wr^{+1}$)	0.00–9.99
MR−1	Image moment log ($\sum wr^{-1}$)	0.00–9.99
R++.....	Image radius in $(+X, +Y)$-direction	0–99
R+−.....	Image radius in $(+X, -Y)$-direction	0–99
R−+.....	Image radius in $(-X, +Y)$-direction	0–99
R−−.....	Image radius in $(-X, -Y)$-direction	0–99
Grad	Maximum image gradient (DN pixel^{-1}) in image	0–999
Lump.....	Dispersion of DN values in image core	0–999
Blend	Identifier for blended image	0–9999
Depth.....	Depth of subdivided blend	0–9999

Note.—DN is the raw image data number (0–255) produced by the camera, and w is DN minus background. The signs of the arguments of the logarithms were saved separately. All quantities were computed for every image and were packed into 52 bytes. The range of values shows the quantization associated with the packing, and not the precision of the calculation. For further details, please consult the source code distributed with the catalog.

in the images is small (perhaps 0.5%) but significant, the choice was made to omit a density-to-intensity calibration and to deal with the images in transmitted light. All of these effects increase the already noisy nature of the photographic emulsion, and tests showed that a least-squares estimator was necessary. In the faint limit, stars look something like a Gaussian, but they have flat cores and wide wings when saturated. The choice was made to use the function

$$T(x, y) = B + \frac{A}{e^{\alpha(r^2 - r_0^2)} + 1}\ , \qquad (1)$$

where $r^2 = (x - x_0)^2 + (y - y_0)^2$. The six free parameters are A (central amplitude), B (background), x_0 and y_0 (position), r_0^2 (saturation radius), and α (extent of image wings). Extensive testing indicated that this symmetric version provided a more stable estimate of the image position than a somewhat better fitting function that includes a seventh free parameter for asymmetry. Traditional nonlinear least-squares based on Marquardt's algorithm (Bevington 1969, p. 235) was used. Iteration was terminated after three steps, regardless of convergence: testing showed that good images were fitted immediately, and that bad images never found a good fit.

The plate-scanning sequence was developed during the testing phase of the PMM program. The first step was to do test exposures and adjust the neutral density filters in the illumination beam to compensate for the background diffuse density of the plate. This was needed because some plates were almost clear, while others were almost black. Next the spatial scanning pattern was done without using the imaging cameras, but while using laser micrometers to measure the distance from the camera to the emulsion. This was needed because plates sagged in the platens, the platens sagged, and some plates had significant ripples in the glass. Once a two-dimensional map of the plate surface was measured, a low-order polynomial was fitted to produce the map that was used during the scanning to keep the CCD a constant distance from the plate. The third step was to focus the cameras by maximizing the sky granularity in the image. The combination of the nominal focus, the map of the plate surface, and the compensation for the background density allowed the scan to commence. Each vision system had an independent prescan sequence, but the scanning of the plates used both cameras whenever possible.

Each platen holds four plates, and typical, out-of-the-Galactic-plane plates took about an hour to scan and produced about 200,000 detections. The slowest plates were in the region of Baade's window, took about 7 hours to scan, and produced more than 7,000,000 detections. The PMM has two platens, and bar codes were placed on all platens, plate envelopes, and magnetic tapes to minimize bookkeeping errors. The hardware and software were frozen at the start of production-mode scanning (1994.7), and it took about 2×10^8 s (1994.7–2001.2) to process essentially all of the almost 19,000 plates involved. About 19×10^{12} pixels were processed (100,000 pixels s^{-1}), and about 15×10^9 detections were logged (75 detections per second). The PMM now sits idle.

4. ASTROMETRIC CALIBRATION

The first step of the calibration takes the pixel coordinates computed in each of the 588 exposures needed to scan a plate, combines them with the metrology of the PMM platen, and produces a catalog of positions in PMM focal-plane coordinates (integer 1×10^{-8} m). It turned out that the elaborate prescan efforts to determine proper focus were not accurate enough, so a numerical refocusing algorithm was developed. This adjusted the coordinates computed in each exposure so as to maximize the number of overlapping-frame multiple detections and to minimize the dispersion in their mean positions. The revision to the focus computed by this algorithm was typically smaller than the focal depth of the camera, but occasionally a plate was found wherein the real-time focus was significantly in error.

The second step was to compute a catalog of astrometric standards for each plate. To the extent enabled by the SLALIB software package (Wallace 1994), the coordinates of stars in this catalog are the apparent position of the star on an idealized Schmidt plate given the circumstances of the observation. The catalog of PMM measures was correlated with these standards, and a cubic transformation was computed.

As is well known, the combination of the Schmidt telescope and the photographic emulsion suffers from large astrometric errors as a function of magnitude. One of the problems with the astrometry presented in USNO-A is that

it used the faintest Tycho-2 stars (Høg et al. 2000) as its astrometric calibrators. While this was the best that could be done at the time, all of these stars are in deep saturation on the survey plates. Hence, the astrometry of faint, unsaturated stars suffered from field-dependent effects that were suspected but uncharacterized at the time USNO-A was compiled. A different strategy was employed for USNO-B. As part of the PMM program, the Northern Proper Motion plates (Klemola, Jones, & Hanson 1987) and the Southern Proper Motion plates (Platais et al. 1998) were scanned, and an astrometric catalog called YS4.0 was compiled. The limiting magnitude of YS4.0 is about $V = 18$, and these stars are not saturated on the Schmidt survey plates. The advantage of this strategy is that the astrometric calibration avoids saturated stars. The disadvantage is that the mean epoch of YS4.0 is about 1975, and the mean motion between YS4.0 and the Schmidt surveys was set to zero by the least-squares solution. Hence, the proper motions in USNO-B are relative, not absolute; future releases of USNO-B will attempt to remove this bias through the introduction of a statistical model.

The first iteration of the astrometric algorithm assumed only a cubic relationship between the plate coordinates and the astrometric standards. Once all of the plates were processed, the astrometric residuals were co-added as a function of position in the focal plane, and the systematic, fixed pattern of astrometric residuals was computed. This was done independently for each survey, and solutions were computed as a function of magnitude and declination. (Declination is a surrogate for zenith distance, since most plates were taken near the meridian.) No obvious correlations with declination were seen, but very large terms and differences in terms were found as a function of magnitude. All of these maps are included in the documentation associated with the digital version of USNO-B, but Figure 1 shows typical maps (POSS-I 103a-O survey at internal PMM magnitudes of $m = 10$ and $m = 18$). For USNO-B, separate maps were used for each survey at each integer internal magnitude between 10 and 19. The map for $m = 10$ was used at all internal magnitudes brighter than 10, and that for $m = 19$ was used for all magnitudes fainter than 19.

Given the maps of fixed-pattern astrometric error, the astrometric solution pipeline was rerun, the maps were included, and the cubic mapping between plate and catalog coordinates was recomputed. Finally, all measures were transformed from plate coordinates to sky coordinates to produce plate-by-plate catalogs of J2000 coordinates at the epoch that the plate was taken.

Although a more thorough analysis of the astrometric accuracy of USNO-B is planned, a coarse estimate can be obtained from the dispersion of the fits for the individual observations (items `Q` and `R` in Table 3). An analysis of the subset of objects with all possible detections (i.e., four in the south and five in the north; about 40% of all objects in USNO-B) shows that the median dispersion is about $0''.12$ in both X and Y. This is an approximate value, and it ignores possible systematic components arising from position on the plate, brightness of the image, or other effects. Users should remember that some USNO-B objects with large astrometric uncertainty may be erroneous combinations of observations of different objects, that the uncertainty in the predicted position of an object increases with time since the mean epoch (often in the 1970s), and that usage of this estimated accuracy should not replace a computation for each object using the values listed in the catalog and the desired epoch of observation.

5. PHOTOMETRIC CALIBRATION

The photometric calibration of the USNO-B catalog is of marginal quality and will be revised as the appropriate data become available. The root of the problem is that an all-sky

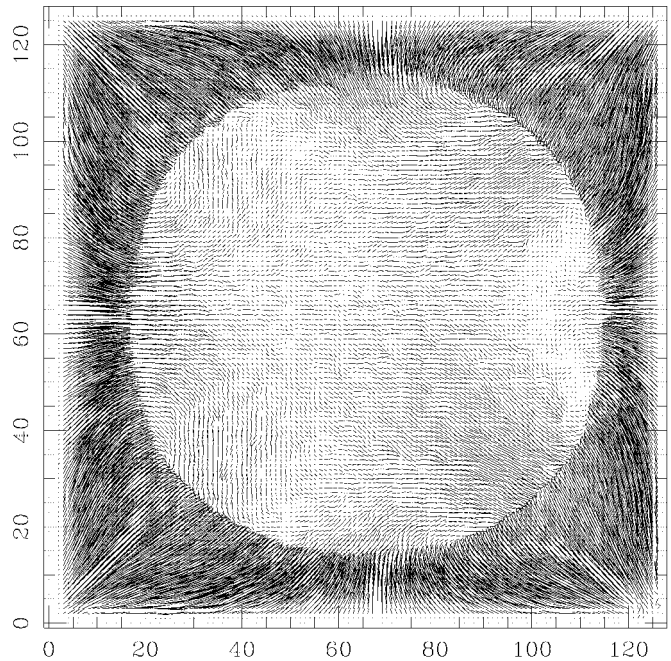

FIG. 1*a*

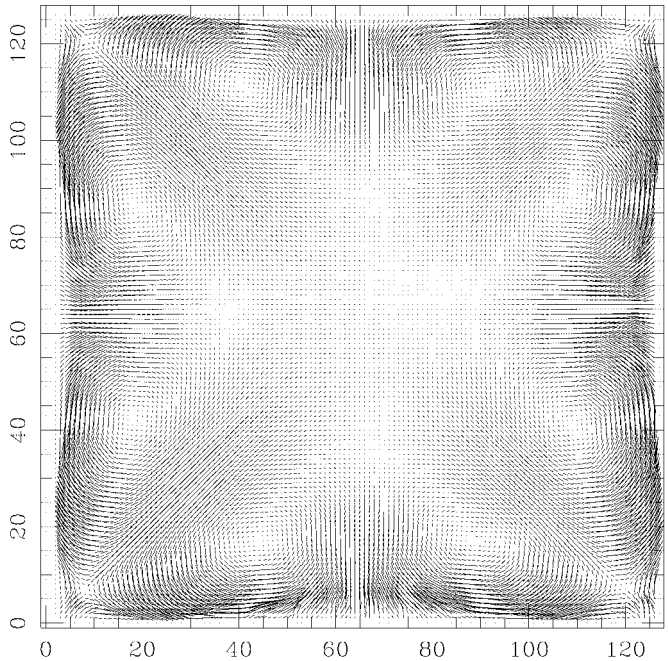

FIG. 1*b*

FIG. 1.—Maps of fixed-pattern astrometric residuals for the mean POSS-I O survey plate at (*a*) 10th and (*b*) 18th magnitude. The diagrams are labeled in bins of 5 mm width, and the mean residuals are scaled such that $0''.20$ is the spacing between bins.

TABLE 3

DATA FOR EACH ENTRY IN USNO-B

Bytes	Packing[a]	Field	Description	Quanta	Decimal Range
0–3	aaaaaaaaa	...	J2000 epoch 2000.0 R.A.	0.″01	0.″00–1,295,999.″99
4–7	sssssss	...	J2000 epoch 2000.0 SPD	0.″01	0.″00–648,000.″00
		AAAA	μ_{RA}[b]	0.″002 yr^{-1}	$-10.''000$ to $+9.''998$ yr^{-1}
		SSSS	μ_{SPD}[b]	0.″002 yr^{-1}	$-10.''000$ to $+9.''998$ yr^{-1}
		P	Total μ probability	0.1	0.0–0.9
8–11	iPSSSSAAAA	i	Motion catalog flag: 0 = no, 1 = yes[c]		
		xxx	$\sigma_{\mu_{RA}}$[b]	0.″001 yr^{-1}	0.″000–0.″999 yr^{-1}
		yyy	$\sigma_{\mu_{SPD}}$[b]	0.″001 yr^{-1}	0.″000–0.″999 yr^{-1}
		Q	$\sigma_{RA\,fit}$[b]	0.″1	0.″0–0.″9
		R	$\sigma_{SPD\,fit}$[b]	0.″1	0.″0–0.″9
		M	Number of detections	...	2–5[d]
12–15	jMRQyyyxxx	j	Diffraction spike flag: 0 = no, 1 = yes[e]		
		uuu	σ_{RA}[b]	0.″001	0.″000–0.″999
		vvv	σ_{SPD}[b]	0.″001	0.″000–0.″999
		eee	Mean epoch minus 1950.0	0.1 yr	1950.0–2049.9
16–19	keeevvvuuu	k	YS4.0 correlation flag: 0 = no, 1 = yes[f]		
		mmmm	First blue magnitude	0.01 mag	0.00–99.99 mag
		FFF	First blue field	...	1–937[g]
		S	First blue survey	...	0–9[h]
20–23	GGSFFFmmmm	GG	First blue star/galaxy	...	0–11[i]
24–27	GGSFFFmmmm	Same as above, but for first red survey			
28–31	GGSFFFmmmm	Same as above, but for second blue survey			
32–35	GGSFFFmmmm	Same as above, but for second red survey			
36–39	GGSFFFmmmm	Same as above, but for N survey			
		RRRR	First blue ξ residual[b]	0.″01	$-50.''00$ to $+49.''99$
		rrrr	First blue η residual[b]	0.″01	$-50.''00$ to $+49.''99$
40–43	CrrrrRRRR	C	Source of photometric calibration		0–9[j]
44–47	CrrrrRRRR	Same as above, but for first red survey			
48–51	CrrrrRRRR	Same as above, but for second blue survey			
52–55	CrrrrRRRR	Same as above, but for second red survey			
56–59	CrrrrRRRR	Same as above, but for N survey			
60–63	iiiiiii	...	First blue look-back index into PMM scan file		
64–67	iiiiiii	Same as above, but for first red survey			
68–71	iiiiiii	Same as above, but for second blue survey			
72–75	iiiiiii	Same as above, but for second red survey			
76–79	iiiiiii	Same as above, but for N survey			

NOTE.—To preserve a fixed-length record for an arbitrary set of detections, the fields associated with a missing survey in the three survey-dependent segments (bytes 20–39, 40–59, 60–79) are set to zero. The number of nonzero entries in each segment will agree with the number of detections M contained in bytes 12–15. Tycho-2 star entries have the same length and a similar (but not identical) format.

[a] Fields seen when the packed integer is printed as a base-10 integer. Combinations of integer division and subtraction are used to extract a particular field.

[b] The calculation for position and motion is done in the tangent plane using the standard coordinates ξ and η with the mean position taken as the tangent point. This is an approximation and will be incorrect for the most demanding of applications.

[c] Objects with large proper motions were cross-correlated with the LHS (Luyten 1979a) and NLTT (Luyten 1979b) Catalogues and the Lowell Proper Motion Survey (Giclas, Burnham, & Thomas 1971, 1978). This flag is set if the USNO-B detection has a correlation in any of these catalog, but the data presented are from the PMM and not from the proper-motion catalog.

[d] M = 0 denotes Tycho-2 stars; M = 1 objects are omitted from USNO-B but saved in the catalog of rejects.

[e] Diffraction spikes from bright stars cause spurious PMM detections. Occasionally, these will correlate to produce a spurious object. The distance to and bearing of the nearest Tycho-2 star was computed, and the flag is set if the distance is within 5 times the radius computed by King & Raff 1977 and the bearing is within 5° of the cardinal points (0°, 90°, 180°, and 270°).

[f] Object was correlated with an object in the YS4.0 catalog (Monet 2003) and therefore contributes in the solution for the mean proper motion of the field.

[g] Field number in original survey ,as shown in Table 1.

[h] Surveys encoded as (0) POSS-I O; (1) POSS-I E; (2) POSS-II J; (3) POSS-II F; (4) SERC-J or SERC-EJ; (5) ESO-R or SERC-ER; (6) AAO-R; (7) POSS-II N; (8) SERC-I; (9) POSS-II N field number but plate taken as part of SERC-I.

[i] The star/galaxy estimator is a measure of the similarity of the image to a stellar point-spread function. Zero means quite dissimilar, and 11 means quite similar.

[j] Photometric calibration source: (0) bright photometric standards on plate; (1) faint photometric standards zero plates away (i.e., on this plate); (2) faint photometric standards one plate away (i.e., on overlap plate); (3) faint photometric standards two plates away (i.e., on overlap of overlap plate), etc.

catalog of faint photometric standards does not exist. Because of this, a two-step photometric calibration strategy was adopted. The first step was to calibrate the bright stars on all of the plates. Tycho-2 stars are almost all brighter than $V = 13$, and although the images are grossly saturated, an almost linear relationship exists between the internal magnitudes measured by the PMM and values computed from spectral energy distributions and the BV magnitudes listed in the catalog. Details of the modeling are presented in the documentation accompanying the digital version of the USNO-B catalog, and A. A. H.'s file tables.txt contains the results. Since Tycho-2 stars are measured on all plates, the bright-star fit was extrapolated and applied to all PMM measures from that plate.

The remaining task was to compute the systematic differences between the true calibration for faint stars and the extrapolation of the bright-star fit. Two sources of photometry for faint stars (magnitudes from 14 to 22) were used, the Guide Star Photometric Catalog 2 (Bucciarelli et al. 2001) and the photometric data measured for the NOFS CCD parallax program (Monet et al. 1992). A. A. H.'s tables were used to convert between the standard-system magnitudes and the photographic magnitudes, and the combination of these two catalogs provided faint standards on 3281 plates, or about 44% of the total needed. Polynomial fits (linear or cubic as necessary) were computed, and the calibrated magnitudes for all objects were obtained.

For the remaining 56% of the plates without faint photometric calibrators, the calibration was computed from the plate overlap zones. The plates adjacent to an uncalibrated plate were searched, and if any had a faint calibration, then it was identified as a possible calibrator and the distance between plate centers was tallied. After searching all nearby plates, the closest one was found, and if there were more than 500 objects in common a calibration was computed. There were 3517 (about 47%) uncalibrated plates that were adjacent to calibrated plates, but three more steps were needed to complete the calibration of all plates. No analysis of all possible overlap regions was done, and this is an area wherein improvements are anticipated in future releases of USNO-B.

It is difficult to give a single number for the photometric accuracy of USNO-B, but the solution combining all 632,827 calibration stars spread over 3281 plates has a standard deviation of 0.25 mag. This value includes whatever effects might arise from the transformation of $BVRI$ to O, E, J, F, N colors, but a similar value is found for each of the 10 different surveys taken separately. Many plates, particularly those calibrated with the photometry from the NOFS parallax program, show substantially smaller errors, and solutions for plates without photometric calibrators may be worse.

Another major problem with USNO-B photometry is that a separate calibration for the photometry of extended objects was not done. In part, this is due to the relatively few catalogs of galaxy photometry. Another factor is that the transformation from magnitudes in a standard system to those in the photographic bandpasses is even less well determined than for stars. The final reason was that the photometric response of the plates is quite nonlinear, and no attempt was made to compute the transformation between the observed values of transmitted light and the true intensity incident on the plate. Whereas the photometry of stars may be useful, the USNO-B magnitudes for nonstellar objects are qualitative, at best.

6. STAR-GALAXY SEPARATION

Although commonly called star-galaxy separation, the value presented in USNO-B is a measure of the similarity of the unknown object to a stellar point-spread function (PSF). Most objects that are dissimilar to the PSF are galaxies, but many other types of astronomical objects and photographic artifacts can produce entries in the catalog. Since the measured transmission was not converted to a true intensity, and because the photographic process is inherently nonlinear, the stellar PSF varies with apparent brightness and position in the focal plane.

The method used to distinguish stars from nonstellar objects was an oblique decision tree with three nodes. Each node of the decision tree is a plane defined by values of two image description parameters, and six (not necessarily distinct) image parameters are needed to define this tree. A decision tree must be trained on a set of objects of known type (star or galaxy). The training set in the northern sky was chosen to be the plates containing the Coma cluster of galaxies. The training set was compiled by hand by examining CCD frames of the Coma Cluster from the KPNO 4 m taken in good seeing by Secker & Harris (1997). The catalog of Coma Cluster galaxies by Godwin, Metcalfe, & Peach (1983) was also consulted. Because of the nonlinearities in the image in transmitted light, each interval of 1 internal magnitude was searched for the set of six image description parameters that provided best star-nonstar discrimination out of the entire set (see Table 2).

Once the training plate of each northern survey was calibrated, the edges of the stellar ridgelines of the various image parameters were identified in five annular zones centered on the plate center. For each of the other plates in the survey, the stellar ridgelines of the relevant parameters were mapped (shift and stretch only) to those of the training plate zone by zone, and the classification index was computed for each object. The calibration of the southern sky was done in a similar manner, but the training set was taken to be a particularly good plate in the equatorial overlap zone, and truth was taken to be the classification from the northern plates. The largest source of classification error is the inability to match the stellar ridgeline on a given plate to that on the training plate.

The classifier produces an integer in the range 0–11 that measures the similarity of the unknown object to a stellar PSF. Values of 0–3 are probably nonstellar, and values of 8–11 are probably stellar. The catalog gives the individual classifications from all surveys other than those taken on IV-N emulsions (see Table 3, bytes 20–39). Various internal tests suggest that the classifier is correct about 85% of the time for objects with internal magnitudes 14–20, but a thorough discussion of the classifier, estimates for its accuracy, and a suggested algorithm for combining the individual estimators for a single object is being prepared.

7. CATALOG COMPILATION

The first phase of the compilation of the final catalog is to apply the astrometric and photometric calibrations to the raw files produced by the PMM in real time. The second phase is to go from a plate-based approach to files having a

constant width in south polar distance (SPD $= \delta + 90^\circ$). It would have been nice to have preserved the 7.°5 width used in the USNO-A catalog, but the size of USNO-B required using a width of 0.°1. The 7435 plate files are written into 1800 SPD files, and then each SPD file is sorted on right ascension. The third phase is to examine the SPD files so that the ensemble of individual observations is reformatted into a list of objects with from one to five observations per object. This task is difficult because there are different numbers of surveys as a function of SPD, there can be duplicate detections of the same object if it fell in a plate overlap zone, and the epoch difference between plates is highly variable. The current algorithm is the following, but modifications may be needed in future releases of USNO-B:

The first step is to find objects that do not move. A 3.″0 aperture is moved through the observation file for a single band of SPD, and an object is sensed when one or more observations are found within the aperture. The list of observations is examined and culled, and all single-observation objects are ignored. If an object contains observations from one or more first-epoch and one or more second-epoch surveys (see Table 1 for assignments), then the object is tallied and the individual observations are removed from further consideration.

The second step is to look for objects with significant proper motions that were observed at all available epochs. The list of objects is recomputed, omitting those that were flagged as no-motion objects, but with the aperture at 30″. For each object, all combinations of second-epoch observations are fitted for linear motion. If significant, the fit is extrapolated to the first-epoch survey(s), and a search is made for detections inside the error ellipse(s). All possible combinations are pursued. If the fit includes all available surveys, has a standard deviation less than 0.″4 in the tangent-plane coordinates ξ and η, and has a motion less than 10″ (five observations), 3″ (four observations), or 1″ (three observations) per year, the detection is tallied and the observations are removed from further consideration.

The third step is to collect reasonable combinations of the remaining detections into objects. The object aperture is set to 20″, and all possible combinations of five-, four-, three-, and two-survey objects are evaluated, in that order. The first collection of observations that has a standard deviation less than 5″ in both ξ and η is called an object, the object is tallied, and the observations are removed from further consideration. Only a few percent of the objects in USNO-B come from this step, and the uncertainty estimators in the catalog should be sufficient to identify them.

In all cases, the combination of individual observations into a single object with proper motion was made without any reference to the individual magnitudes. Since more than 200 billion (2×10^{11}) possible combinations were considered, there may be spurious merges in the catalog. For many applications, a test on the individual magnitudes can be used to identify catalog entries that may be erroneous combinations of different objects.

The final step is to remove double detections and to replace bright stars. Double detections occur because the zones of SPD used during the compilation are somewhat wider than 0.°1 in order to allow for edge effects. King & Raff (1977) give values for the relationship between image diameter and apparent magnitude on POSS-I plates. Mean values were used for all surveys to remove all PMM detections near Tycho-2 stars, since the PMM's measures are usually confused by the gross saturation, diffraction spikes, and halos. After removing the PMM detections, the reformatted Tycho-2 entry is inserted for completeness.

Table 3 gives the data contained in USNO-B for each object. The catalog is organized into 1800 zones of SPD, each exactly 0.°1 in width, and the objects are sorted by right ascension in each zone. In addition, accelerator files for each zone contain the first entry and number of entries at each increment of $15^{\rm m}$ of right ascension. As was found with USNO-A, these files increase the efficiency of catalog access. Users who need a more detailed description are urged to read the documentation and the source code distributed with the catalog. The overriding concerns were to include as many objects as is reasonable (since the alternative is to omit the associated detections) and to require spatially correlated detections on any two or more surveys (even if the combinations may seem curious). At NOFS, the list of remaining observations has been saved and will be served to users upon special request.

8. COMPARISON WITH THE SDSS EARLY DATA RELEASE

In an effort to substantiate the internal uncertainty estimators, the $\sim$450 deg^2 of the Sloan Digital Sky Survey (SDSS) Early Data Release (EDR; Stoughton et al. 2002) were correlated with USNO-B1.0. The SDSS results are based on CCD data and have substantially smaller uncertainties than the observations from which USNO-B was compiled. The astrometric comparison for objects determined by SDSS to be unblended and in the magnitude range $17 < g^* < 19$ shows a dispersion of about 0.″13 for stars and 0.″20 for galaxies. Unfortunately, systematic offsets as large as 0.″25 were found, and these are taken as evidence of distortions in the USNO-B1.0 astrometric calibration. Comparison of the stellar photometry in the magnitude range of 15–21 yields the following transformations and dispersions:

$$\mathrm{O} = g^* + 0.08 + 0.452(g^* - r^*), \quad \sigma = 0.34\ , \qquad (2a)$$

$$\mathrm{E} = r^* - 0.20 - 0.086(g^* - r^*), \quad \sigma = 0.30\ , \qquad (2b)$$

$$\mathrm{J} = g^* + 0.06 + 0.079(g^* - r^*), \quad \sigma = 0.33\ , \qquad (2c)$$

$$\mathrm{F} = r^* - 0.09 - 0.109(g^* - r^*), \quad \sigma = 0.26\ , \qquad (2d)$$

$$\mathrm{N} = i^* - 0.44 - 0.164(r^* - i^*), \quad \sigma = 0.31\ . \qquad (2e)$$

These relations were determined from the 34 POSS-I fields and the 40 POSS-II fields that are covered by the SDSS EDR, so they represent only a small fraction of the USNO-B catalog. Examination of the residuals from these relations suggests that there are additional systematic errors that depend on magnitude, up to 0.15 mag, and that vary from plate to plate, up to 0.2 mag for red plates and somewhat worse for blue plates. Little systematic variation ($\leq$0.1 mag) is seen with distance from the center of a plate.

Figure 2 displays the fraction of SDSS objects with matching USNO-B entries (within a radius of 1″, after applying USNO-B proper motions to convert USNO-B positions to the epoch of the SDSS observations) as a function of SDSS g^* magnitude. USNO-B is essentially 100% complete for stars determined to be unblended with other objects by SDSS, but the completeness drops to about 97%

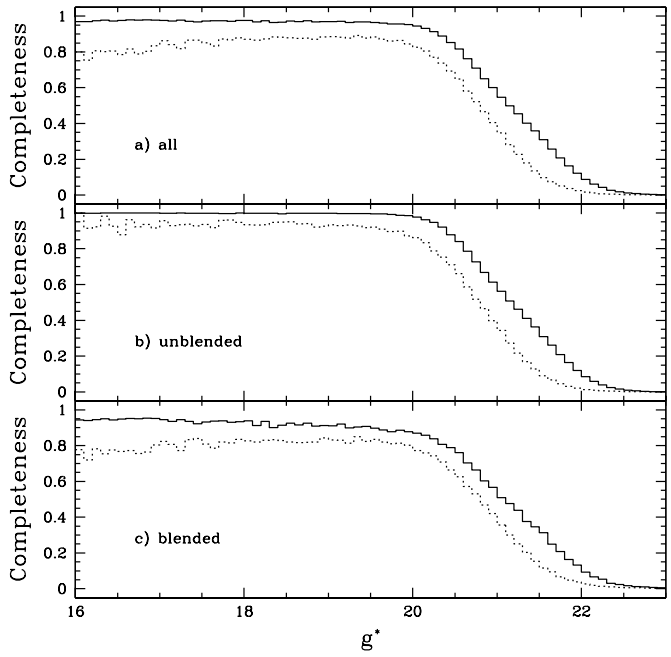

FIG. 2.—Fraction of SDSS objects detected by USNO-B as a function of SDSS g^* magnitude. The solid and dotted lines are for objects classified by SDSS as stars and galaxies, respectively. (*a*) All objects; (*b*) objects determined to be unblended by SDSS; (*c*) objects determined to be blended with other objects by SDSS.

when all SDSS objects are considered. This is yet more evidence that CCD data are far superior for image deconvolution than those obtained from photographic plates. USNO-B is roughly 92% complete for unblended SDSS galaxies with $g^* < 19.5$. Table 4 shows the correlation between USNO-B and SDSS classifications as a function of SDSS g^* magnitude. These accuracies are nominal, since accuracy variations exist from plate to plate and from magnitude interval to magnitude interval on a given plate.

9. CAVEATS AND CONCLUSIONS

USNO-B is a work in progress, and the version 1.0 public release is a compromise between the needs of the community and the development and testing of the catalog compilation software. There are systematic errors and other problems, and future revisions will attempt to address these. Because of the catalog's size, human verification of every entry cannot be done. Many of the verification algorithms are statistical in nature, and this leaves open the possibility for small and large errors in specific areas. The following, incomplete list of caveats should serve as a warning to the users of the catalog of the types of difficulties encountered, and the need for skepticism in believing the attributes of peculiar entries:

The photometric calibration is preliminary. Only 44% of the fields have faint calibrators somewhere on the plate, and in many cases there are only a very few of these. There is no separate calibration of the magnitudes of nonstellar objects, so these should be treated as qualitative measures. The catalog presents magnitudes in the photographic systems (O, E, J, F, N) and not on standard systems, to minimize uncertainties and the chances for systematic errors. A vignetting function for the Schmidt telescopes has not been studied beyond preliminary tests that showed it was probably unimportant. Photometry is probably the weakest aspect of USNO-B and will be the subject of the most work in the future.

Please do not ignore the proper motions. The catalog lists the positions for objects in J2000 at the epoch 2000.0, and in many cases this epoch is more than 25 years away from the mean epoch of the observations. Errors in the proper motion, or errors in assigning particular observations to the same object that give rise to spurious proper motions, produce catalog positions for patches of empty sky. If you wish to ignore the true proper motion, you should use the catalog motions to compute the position at the mean epoch and use this position instead of the 2000.0 position. This is particularly important for objects with large proper motions ($\mu \geq 1''.0$ yr^{-1}). The epoch difference of the plate material in a single field can often be as large as 50 years. Allowing the software to use a large search radius greatly increases the probability of spurious detections, but limiting the search radius to a small value will remove all real high proper motion objects from the catalog. Users should understand that the reality of grouping observations into a single object with high proper motion is a strong function of the number and epoch of the individual observations. Extreme caution is suggested for all such objects, particularly those that are missing one or more opportunities for detection because of faint magnitude or extreme color.

USNO-B presents relative, not absolute, proper motions. The calibration process described above sets the mean

TABLE 4
AGREEMENT BETWEEN USNO-B AND SDSS IMAGE CLASSIFICATION

Survey	$g = 13$	$g = 14$	$g = 15$	$g = 16$	$g = 17$	$g = 18$	$g = 19$	$g = 20$	$g \geq 21$
188,515 Stars									
POSS-I O	0.50	0.81	0.78	0.93	0.96	0.88	0.74	0.49	0.31
POSS-I E	0.67	0.85	0.84	0.97	0.96	0.95	0.92	0.80	0.53
POSS-II J.....	0.50	0.80	0.84	0.89	0.92	0.92	0.79	0.55	0.37
POSS-II F	1.00	0.97	0.93	0.94	0.95	0.93	0.78	0.59	0.52
172,020 Galaxies									
POSS-I O	0.24	0.36	0.88	0.92	0.89	0.95	0.76	0.71	0.75
POSS-I E	0.33	0.33	0.84	0.82	0.82	0.87	0.85	0.82	0.86
POSS-II J.....	0.17	0.21	0.89	0.96	0.91	0.83	0.83	0.85	0.84
POSS-II F	0.21	0.25	0.84	0.94	0.91	0.83	0.91	0.90	0.88

motion of all objects correlated with entries in the YS4.0 catalog to be zero. Since least-squares was used, the solution is dominated by large numbers of faint stars, and it is believed that the mean correlated star is between yellow magnitudes of 17 and 18. Whereas this motion may be small in absolute terms, it may be significant in various statistical studies. Future releases of USNO-B will attempt to minimize or remove this bias.

USNO-B covers the entire sky, and users should understand that there are many areas of the sky that do not resemble sparse, high Galactic latitude fields where objects are isolated and the sky is well defined. In dense fields, the sky is only poorly determined, and the PMM often counted more than 5 million distinct objects on a Schmidt plate. Users should understand that photographic photometry and astrometry are not well defined in such regions, nor are they well defined in regions of nebulosity, near well-resolved objects such as globular clusters and bright galaxies, or around bright stars. The "any two" rule for merging observations from individual surveys into objects arose from the desire to retain faint blue or faint red objects that were omitted from USNO-A, but the penalty is to increase the probability of false objects in peculiar regions of sky. USNO-B data should not be used for the study of such regions: $67'' \text{ mm}^{-1}$ is a very coarse scale, the dynamic range of plates is limited, and PSF reconstruction with multi-PSF image deconvolution was not done. Again, this catalog is based on photographic data, and these are of lower quality than those that are familiar to younger astronomers.

Please do not use USNO-B as a source of data for bright stars. For the sake of completeness and the minimization of confusion, holes were cut around Tycho-2 stars and the Tycho-2 data were copied into the catalog. The original Tycho-2 data should be used for all critical applications. Stars within a few magnitudes of the Tycho-2 limiting magnitude are saturated on the Schmidt plates, and astrometric and photometric values are of lower accuracy.

USNO-B is one of the few attempts to digitize, process, and analyze the entire sky as seen in different optical colors and at different epochs, and it contains successes and failures. It is an all-sky catalog of positions, proper motions, magnitudes, and classifications for more than a billion objects, and its accuracy is about $0''.2$ for astrometry, 0.3 mag for photometry, and 85% for object classification. As demonstrated by comparison with the SDSS EDR and other zone catalogs, systematic astrometric and photometric errors exist in this version, and there may be large regions of sky wherein the automated verification algorithms failed without signaling an error. The release of USNO-B1.0 is a compromise between the desire for public access and the process of catalog compilation and verification. The next step in the USNO-B process will be to join the database with the Two Micron All Sky Survey (Skrutskie et al. 1997),[7] and this will entail a top-to-bottom verification and recalibration of the USNO-B algorithms. The scheduled release date for USNO-B1.1 is 2003 September. As was USNO-A, USNO-B is just a milestone in the processing of the PMM's archive. Future work will be directed toward finding a way to calibrate the data from all of the plates that the PMM has scanned and to identify a method to make these available to the community. Manpower and costs are finite, but the quality and importance of the historic photographic data justify these efforts.

The first, and probably the most important, acknowledgment goes to the many individuals (observers, technicians, assistants, graduate students, etc.), mostly anonymous except in biodegrading paper logs and documents, whose dedication and expertise have produced the stunning collection of plates that the PMM had the privilege of scanning. The record of the sky is irreplaceable, and that it is of such high quality serves as an inspiration to those who follow in their footsteps. Most of the errors and inaccuracies in USNO-B belong to the PMM, and not to the original archive.

Although technically in the public domain and hence requiring no acknowledgment, it is appropriate to repeat these sentences from Minkowski & Abell (1963):

> The Sky Survey was made financially possible by grants from the National Geographic Society. The society provided the photographic materials and special equipment required, the salaries of the personnel employed full- or part-time on the survey, and the production of the two sets of contact positives on glass of each survey photograph. The observing time with the 48 inch Schmidt telescope required to obtain the Sky Survey photographs was made available by the Palomar Observatory of the California Institute of Technology.

This work is based partly on photographic plates obtained at the Palomar Observatory 48 inch Oschin Telescope for the Second Palomar Observatory Sky Survey, which was funded by the Eastman Kodak Company, the National Geographic Society, the Samuel Oschin Foundation, the Alfred Sloan Foundation, National Science Foundation grants AST 84-08225, 87-19465, 90-23115, and 93-18984, and National Aeronautics and Space Administration grants NGL 05-002-140 and NAGW-1710.

Some of the measures used in the USNO-B catalog are based on photographic data obtained using the UK Schmidt Telescope. The UK Schmidt Telescope was operated by the Royal Observatory Edinburgh, with funding from the UK Science and Engineering Research Council, until 1988 June, and thereafter by the Anglo-Australian Observatory. Original materials are copyrighted by the Royal Observatory Edinburgh and the Anglo-Australian Observatory, and the plates were scanned with their permission.

Thanks are expressed to the European Southern Observatory (ESO) for permission to scan the ESO-R survey glass plate copies housed at the National Optical Astronomy Observatory. ESO retains copyright and other intellectual property rights to these plates. Special thanks are extended to those at the California Institute of Technology, Royal Observatory Edinburgh, and the Anglo-Australian Observatory for the loan of original plate material, and to the National Optical Astronomy Observatory for loaning their collection of glass copies.

The continuing support of the US Air Force, particularly HQ AFSPC/DOY (and predecessors) and Joseph Liu, is greatly appreciated. It is rare to see such a successful combination of mission, operational, and scientific goals.

[7] See http://www.ipac.caltech.edu/2mass.

B. C. is grateful to Jeff Secker for providing invaluable high-resolution digital imaging of the Coma Cluster, with which the training set for the image classifier was constructed.

Funding for the creation and distribution of the SDSS Archive has been provided by the Alfred P. Sloan Foundation, the Participating Institutions, the National Aeronautics and Space Administration, the National Science Foundation, the US Department of Energy, the Japanese Monbukagakusho, and the Max-Planck-Gesellschaft. The SDSS Web site is http://www.sdss.org/. The SDSS is managed by the Astrophysical Research Consortium for the Participating Institutions. The Participating Institutions are the University of Chicago, Fermilab, the Institute for Advanced Study, the Japan Participation Group, Johns Hopkins University, Los Alamos National Laboratory, the Max-Planck-Institut für Astronomie, the Max-Planck-Institut für Astrophysik, New Mexico State University, the University of Pittsburgh, Princeton University, the US Naval Observatory, and the University of Washington.

REFERENCES

Bevington, P. R. 1969, Data Reduction and Error Analysis for the Physical Sciences (New York: McGraw-Hill)
Bucciarelli, B., et al. 2001, A&A, 368, 335
Giclas, H. L., Burnham, R., Jr., & Thomas, N. G. 1971, Lowell Proper Motion Survey, Northern Hemisphere (Flagstaff: Lowell Obs.)
———. 1978, Lowell Proper Motion Survey: Southern Hemisphere Catalog (Flagstaff: Lowell Obs.)
Godwin, J. G., Metcalfe, N., & Peach, J. V. 1983, MNRAS, 202, 113
Høg, E., et al. 2000, A&A, 355, L27
King, I. R., & Raff, M. I. 1977, PASP, 89, 120
Klemola, A. R., Jones, B. F., & Hanson, R. B. 1987, AJ, 94, 501
Luyten, W. J. 1979a, LHS Catalogue (2d ed.; Minneapolis: Univ. Minnesota)
———. 1979b, NLTT Catalogue (Minneapolis: Univ. Minnesota)
Minkowski, R., & Abell, G. O. 1963, in Stars and Stellar Systems, Vol. 3, Basic Astronomical Data, ed. K. A. Strand (Chicago: Univ. Chicago Press), 481
Monet, D., et al. 1994, UJ1.0 (Flagstaff: US Nav. Obs.)
———. 1996, USNO-A1.0 (Flagstaff: US Nav. Obs.)
———. 1998, USNO-A2.0 (Flagstaff: US Nav. Obs.)
Monet, D. G., Dahn, C. C., Vrba, F. J., Harris, H. C., Pier, J. R., Luginbuhl, C. B., & Ables, H. D. 1992, AJ, 103, 638
Morgan, D. H., Tritton, S. B., Savage, A., Hartley, M., & Cannon, R. D. 1992, in Digitised Optical Sky Surveys, ed. H. T. MacGillivray & E. B. Thomson (Dordrecht: Kluwer), 11
Platais, I., et al. 1998, AJ, 116, 2556
Secker, J., & Harris, W. E. 1997, PASP, 109, 1364
Skrutskie, M. F., et al. 1997, in The Impact of Large Scale Near-IR Sky Surveys, ed. F. Garzón, N. Epchtein, A. Omont, W. B. Burton, & P. Persi (Dordrecht: Kluwer), 25
Stoughton, C., et al. 2002, AJ, 123, 485 (erratum 123, 3487)
Wallace, P. T. 1994, in ASP Conf. Ser. 61, Astronomical Data Analysis Software and Systems III, ed. D. R. Crabtree, R. J. Hanisch, & J. Barnes (San Francisco: ASP), 481